JOURNAL OF AGRICULTURAL AND FOOD CHEMISTRY
ARTICLE

J. Agric. Food Chem. 2010, 58, 5649–5657 5649
DOI:10.1021/jf9045396

Isolation, Expression, and Characterization of a 13-Hydroperoxide Lyase Gene from Olive Fruit Related to the Biosynthesis of the Main Virgin Olive Oil Aroma Compounds

María N. Padilla, M. Luisa Hernández, Ana G. Pérez, Carlos Sanz,* and José M. Martínez-Rivas

Department of Physiology and Technology of Plant Products, Instituto de la Grasa, Consejo Superior de Investigaciones Científicas (CSIC), Avenida Padre García Tejero 4, 41012 Seville, Spain

A full-length cDNA clone (*OepHPL*) coding for hydroperoxide lyase was isolated from olive fruit (*Olea europaea* cv. Picual). The deduced amino acid sequence shows significant similarity to known plant hydroperoxide lyases and contains a N-terminal sequence that displays structural features of a chloroplast transit peptide. Genomic Southern blot analysis indicates that at least one copy of *OepHPL* is present in the olive genome. The recombinant hydroperoxide lyase was specific for 13-hydroperoxide derivatives of linolenic and linoleic acids but did not use 9-hydroperoxy isomers as substrates. Analyses of reaction products revealed that this enzyme produces primarily (*Z*)-hex-3-enal, which partially isomerizes to (*E*)-hex-2-enal, from 13-hydroperoxylinolenic acid and hexanal from 13-hydroperoxylinoleic acid. Expression levels were measured in different tissues of Picual and Arbequina varieties, including mesocarp and seed during development and ripening of olive fruits. The involvement of this olive hydroperoxide lyase gene in the biosynthesis of virgin olive oil aroma compounds is discussed.

KEYWORDS: ***Olea europaea*; gene expression; hydroperoxide lyase; olive oil; volatiles**

INTRODUCTION

Hydroperoxide lyases (HPLs) catalyze the cleavage of polyunsaturated fatty acid hydroperoxides to aldehydes and oxoacids. These aldehydes play a major role in forming part of the aroma profile of many plant fruits and flowers. In addition, they have antimicrobial activity *in vitro* and thus are thought to be involved in the plant defense response against pest and pathogen attack (*1*). Moreover, HPL-catalyzed production of six straight-chain carbon (C6) aldehydes may be a key step of a built-in resistance mechanism of plants against some sucking insect pests (*2*), and it is also discussed that they are a part of the volatile mixture that attracts predators upon herbivore attack (*3*).

HPLs belong to a novel family of cytochrome P450s (CYP74) that, unlike other P450 enzymes, do not require molecular oxygen nor NAD(P)H-dependent cytochrome P450 reductase as cofactors, using polyunsaturated fatty acid hydroperoxides as both the substrate and oxygen donor. All members of the CYP74 family synthesize oxilipins as participants of the different branches of the lipoxygenase (LOX) pathway, and on the basis of sequence identity, they are divided into four subfamilies: CYP74A (allene oxide synthase), CYP74B (13-HPLs), CYP74C (9/13-HPLs), and CYP74D (divinyl ether synthase) (*4*). Moreover, on the basis of their substrate preference, enzymes with HPL activity are divided into three groups: 13-HPLs, such as those from tea leaves (*5*), watermelon (*6*), or tomato leaves (*7*), having a strong preference for 13-hydroperoxides, HPLs accepting either 9- or 13-hydroperoxides as the substrate (9/13-HPLs), including those from cucumber fruit and seedlings (*8*) or alfalfa seedlings (*9*), and 9-HPL, active specifically on 9-hydroperoxides of polyunsaturated fatty acids, such as HPL from pear fruit (*10*).

Most CYP74 cDNAs encode plastidial transit peptides (*11*). Farmaki et al. (*12*) obtained evidence for a differential distribution of the LOX pathway enzymes within potato leaf chloroplasts, suggesting a possible mechanism to separate physically the different synthetic branches of the LOX pathway.

C6 aldehydes are the most important quantitative and qualitative compounds in virgin olive oil (VOO) aroma (*13*, *14*). These C6 compounds are synthesized *de novo* when enzymes and substrates meet as tissues are disrupted during olive oil processing. The participation of the LOX pathway in the biosynthesis of C6 compounds in olive oil aroma was established by Olias et al. (*15*). These compounds are produced from polyunsaturated fatty acids containing a (*Z*,*Z*)-penta-1,4-diene structure, such as linoleic (LA) and linolenic (LnA) acids. In a first step of this pathway, LOX produces the corresponding 13-hydroperoxide derivatives (*15*−*17*) that are subsequently cleaved by HPL to C6 aldehydes. HPL activity has been characterized in enzymatic extracts from olive fruits, demonstrated to metabolize 13-hydroperoxides of LnA and LA, but shows no activity when 9-hydroperoxides were used as substrates (*15*, *18*).

The biosynthesis of VOO aroma compounds seems to mainly depend upon the availability of non-esterified polyunsaturated fatty acids, especially LnA, and the enzymatic activity of the LOX/HPL system during the industrial oil extraction process (*19*). This process is carried out only by physical methods, involving olive fruit crushing, paste kneading, and oil separation. This product is classified for commercial purposes based on its

*To whom correspondence should be addressed. Telephone: +34-95-4611550. Fax: +34-95-616790. E-mail: carlos.sanz@ig.csic.es.

Published on Web 03/24/2010

chemical and sensory parameters. Sensory analysis is performed through taste and aroma evaluations by certified test panels. Therefore, production of flavorful olive oils is considered a priority in olive-breeding programs. In this sense, the aim of this work was to characterize HPL genes/enzymes from olive fruit. Thus, we have isolated and characterized the first olive *HPL* gene, which codes for an enzyme that exhibits 13-HPL activity. The catalytic properties of this olive HPL are consistent with its involvement in the synthesis of main oil volatile compounds during the industrial process to obtain VOO.

MATERIALS AND METHODS

Chemicals. Culture media components and agarose were purchased from Pronadisa (Torrejón de Ardoz, Spain), and liquid-chromatography-grade solvents and buffer components were supplied by Merck (Darmstadt, Germany). Isopropyl-β-D-thiogalactopyranoside (IPTG), X-Gal, restriction enzymes, RNase A, molecular markers for DNA, and dNTPs were purchased from Fermentas (Vilnius, Lithuania). Fatty acids, soybean LOX, antibiotics, amino acids, and reference compounds used for volatile identification were supplied by Sigma-Aldrich (St. Louis, MO), except for (*Z*)-hex-3-enal generously supplied by S.A. Perlarom (Louvaine-La-Neuve, Belgium).

Plant Material. Olive (*Olea europaea* L. cv. Picual and Arbequina) trees were grown in the experimental orchards of the Instituto de la Grasa, Seville (Spain), with drip irrigation and fertigation from the time of full bloom to fruit maturation. Young drupes, developing seeds, and mesocarps were harvested at different times after bloom corresponding to different developmental stages of the olive fruit, chilled in liquid nitrogen, and stored at −80 °C. Young leaves were collected similarly.

Isolation of a HPL Full-Length cDNA Clone. For isolation of HPL partial cDNA clones, two degenerate primers MN5 (5′-GGGTTYAAY-GCNTWYGGNGG-3′) and MN6 (5′-GTYTSGSKGYCGTTNSWC-CA-3′) were designed from the comparison of known plant HPL amino acid sequences, which correspond to the highly conserved sequences GFNA(F/Y)GG for MN5 and WSN(G/E)(P/R)(Q/E)T for MN6. This pair of primers, together with an aliquot of an olive Uni-ZAP XR cDNA library constructed with mRNA isolated from Picual olive fruits 13 weeks after flowering (WAF) (*20*), was used for polymerase chain reaction (PCR) amplification with the Thermo-Start DNA polymerase (ABgene, Epsom, U.K.). A DNA fragment with the expected size was generated, subcloned into the vector pGEM-T Easy (Promega, Madison, WI), and sequenced.

PCR amplification of the 5′ end and isolation of the full-length cDNA clone were performed according to Hernandez et al. (*21*).

DNA sequencing was performed by GATC Biotech, Konstanz (Germany), and the DNA sequence data were analyzed as previously described (*17*).

Genomic Southern Blot Analysis. Olive genomic DNA was isolated from young leaves by the CTAB method (*22*). Genomic Southern blot analysis was performed using olive genomic DNA samples of 10 μg as previously described (*21*), except that the final wash was performed for 15 min at 45 °C. The olive *HPL* gene-specific probe, corresponding to the 3′ untranslated region (UTR) and with a size of 132 bp, was obtained by PCR amplification with the following pair of specific primers: MN62 (5′-ATGAAGGATGTAATGCTACTC-3′) and MN26 (5′-AAGTAAA-GAATGTCACGCTCC-3′).

Total RNA Extraction and cDNA Synthesis. Total RNA isolation was performed from 1 to 2 g of frozen olive tissues collected from at least three different olive trees as described by Hernandez et al. (*21*). RNA quality verification, removal of contaminating DNA, and cDNA synthesis were carried out according to Hernandez et al. (*23*).

Quantitative Real-Time PCR (qRT-PCR). Gene expression analysis was performed by qRT-PCR as previously described (*23*). Primers for gene-specific amplification of the olive *HPL* gene (Table A in the Supporting Information) were designed from the region of the open reading frame (ORF) preceding the cytochrome P450 domains to avoid detection of other cytochrome P450 enzymes. The housekeeping olive ubiquitine2 gene (*OeUBQ2*, AF429430) was used as an endogenous reference to normalize. The real-time PCR data were calibrated relative to the corresponding gene expression level in 12 WAF mesocarp tissue from Picual for all studied tissues and varieties, following the $2^{-\Delta\Delta Ct}$ method for relative quantification (*24*). The data are presented as means ± standard deviation (SD) of three reactions performed in different 96-well plates, each having two replicates in each plate.

Expression of Olive *HPL* Gene in *Escherichia coli*. The corresponding ORF of the olive *HPL* gene described above, except the sequence of the chloroplast transit peptide, was amplified by PCR using Ecozyme DNA polymerase (Ecogen, Barcelona, Spain), which has proofreading activity, and the following pair of specific primers: MN65, 5′-GTCGGATCC-CTCTGCCCCTCCGCGCCATTCTT-3′, and MN66, 5′-CAGTCAAG-CTTTCACTTGGACTTCTCAACTGCAGTGATTG-3′. The primers were extended by *Bam*HI and *Hind*III restriction sites (underlined) for ligation behind the inducible T7/*lac* promoter of the bacterial expression vector pET21d(+) (Novagen, Germany). This vector provides a start codon, and a T7 tag is added to the N terminus of the HPL protein. The resulting 1.4 kb PCR product was digested with the restriction enzymes and ligated into *Bam*HI- and *Hind*III-digested and dephosphorylated pET21d(+). The *E. coli* strain BL21 (DE3) was transformed with this plasmid and selected on LB ampicillin plates. The complete *OepHPL* ORF of this construct was checked by sequencing prior to the expression studies. LB medium containing ampicillin (6 mL) was inoculated with a single colony of freshly transformed bacteria and grown at 37 °C until the A_{600} was 0.5. Then, 200 mL of LB ampicillin medium were inoculated with the whole preculture and grown at 37 °C. When the culture reached an A_{600} of 0.6, 1 mM IPTG was added to induce gene expression. The culture was subsequently incubated at 25 °C for 15 h. Bacteria were harvested by centrifugation at 2500*g* for 10 min at 4 °C. Cell pellet aliquots corresponding to 50 mL cultures were washed with water, frozen with liquid nitrogen, and kept at −80 °C.

Purification of the Recombinant Enzyme. To obtain the crude extract, the frozen cell pellet was thawed and suspended in 100 mM Na−phosphate buffer at pH 6.7 containing 50 mM Na_2EDTA, 5% (v/v) glycerol, 1% (v/v) Triton X-100, and 2 mg mL^{-1} lysozyme, in a proportion of 2.5 mL of buffer/50 mL of bacterial culture. After 15 min of incubation with orbital shaking at room temperature, the lysate was centrifuged at 10000*g* for 10 min at 4 °C and the supernatant was used as a crude extract. NaCl and KCl were added to the crude extract to make it 137 mM NaCl and 2.7 mM KCl and mixed gently for 15 min at room temperature with 0.5 mL of T7 tag antibody agarose, which had been previously equilibrated with 5 mL of conditioning buffer [100 mM Na−phosphate at pH 6.7, 50 mM ethylenediaminetetraacetic acid (EDTA), 5% (v/v) glycerol, 1% (v/v) Triton X-100, 137 mM NaCl, and 2.7 mM KCl]. The mixture was loaded on an empty column provided with a frit, and the solid phase was washed with 5 mL of conditioning buffer. Elution of HPL protein was performed with 0.1 M citric acid at pH 2.2. Fractions of 1 mL were collected in tubes containing 150 μL of 2 M Tris base at pH 10.4 and assayed for HPL activity.

HPL Assay and Preparation of Fatty Acid Hydroperoxides. Two different methods were used to assay HPL activity. For rapid measurements, HPL activity was assayed spectrophotometrically according to Olias et al. (*15*) by measuring the decrease of A_{234} because of the disruption of the conjugated diene chromophore of the substrates at 25 °C. The 1.5 mL standard assay mixture consisted of 100 mM Na−phosphate buffer at pH 8, 8 μL of 10 mM substrate solution, and 10−20 μL (approximately 1.4 μg of protein) of enzyme solution. One unit (U) of HPL activity is defined as the amount of enzyme catalyzing the formation of 1 μmol of product/min.

For the study of the catalytic properties, HPL activity was tested using a coupled HPL/alcohol dehydrogenase (ADH) method according to Vick (*25*). The enzyme activity was measured using polyunsaturated fatty acid hydroperoxides in the presence of yeast ADH and NADH. The production of aldehydes was measured by monitoring at 25 °C the decrease of A_{338} because of the oxidation of NADH by ADH when reducing HPL products (aldehyde and oxoacid) to alcohols. The 1.5 mL standard assay mixture consisted of 100 mM Na−phosphate buffer at pH 8, 8 μL of 10 mM substrate solution, 20 μL of ADH (50 U), 30 μL of 10 mM NADH, and 10−20 μL (approximately 1.4 μg of protein) of enzyme solution. One unit (U) of HPL activity is defined as the amount of enzyme catalyzing the oxidation of 2 μmol of NADH/min.

The 13- and 9-hydroperoxy isomers from the polyunsaturated fatty acid were prepared using soybean lipoxygenase according to the method of Hamberg and Samuelsson (*26*) or with potato lipoxygenase as described by Galliard and Phillips (*27*), respectively.

Analysis of HPL Reaction Products. Fatty acid hydroperoxide substrate solution (40 μL) was incubated in 1.5 mL of 100 mM Na−phosphate buffer at pH 8 with purified OepHPL (20 mU) for 5 min. The incubation mixture (0.5 mL) was transferred to a vial containing 1.5 mL of saturated $CaCl_2$. The vial was heated at 40 °C, and after 10 min of equilibrium time, volatile compounds from headspace were adsorbed 30 min at 40 °C on a SPME fiber DVB/Carboxen/PDMS 50/30 μm (Supelco Co., Bellefonte, PA). Sampling was carried out in triplicate. Desorption of volatile compounds trapped on the SPME fiber was performed directly into the gas chromatograph (GC) injector. Volatiles were analyzed using a HP-6890 GC−flame ionization detector (FID) equipped with a DB-Wax 20 M (60 m × 0.25 mm inner diameter; film thickness, 0.25 μm; J&W Scientific, Folsom, CA). Operating conditions were as follows: N_2 as carrier gas, gas injector and detector at 250 °C, and column held for 6 min at 40 °C and then programmed at 2 °C min^{-1} to 128 °C. Each separated product was identified by high-resolution gas chromatography−mass spectrometry (HRGC−MS) analysis (Fisons series 8000) performed on a ZB-Wax capillary column (30 m × 0.25 mm inner diameter; film thickness, 0.25 μm; Phenomenex, Torrance, CA), operated at 40 °C for 6 min and then programmed at 2 °C min^{-1} to 128 °C, with MS ionization potential at 70 eV.

Effect of pH and Temperature on Enzyme Activity. Optimal pH for the enzyme activity was measured over a pH range of 4.0−10.0, monitoring the decrease of A_{234} under standard assay conditions. The buffers used were 100 mM Na−acetate buffer (pH 3.6−5.3), 100 mM Na−phosphate buffer (pH 5.5−8.0), and 100 mM Na−borate buffer (pH 8.5−10.0).

The optimal temperature for enzyme activity was determined over a temperature range of 15−60 °C in increments of 5 °C using the same assay conditions.

Protein Determination. Protein was estimated using the Bio-Rad Bradford protein reagent dye with bovine serum albumin (BSA) as the standard.

Olive Oil Extraction. Olive oil extraction was performed using an Abencor analyzer (Comercial Abengoa, S.A., Seville, Spain) simulating the industrial process of VOO production. Milling of olive fruit (batches of 1 kg in duplicate experiments) was performed using a stainless-steel hammer mill operating at 3000 rpm provided with a 5 mm sieve. Resulting olive pastes were immediately submitted to kneading in a mixer at 50 rpm for 30 min at 30 °C. Centrifugation of the kneaded olive pastes was performed in a basket centrifuge at 3500 rpm for 1 min. After centrifugation, oils were decanted and paper-filtered. Samples for volatile analyses (0.5 g) were transferred to 10 mL septum vials, sealed under N_2, and stored at −18 °C until analysis.

Analysis of Volatile Compounds. Olive oil samples were conditioned to room temperature and then placed in a vial heater at 40 °C. After 10 min of equilibrium time, headspace volatiles were adsorbed 50 min at 40 °C on a SPME fiber DVB/Carboxen/PDMS 50/30 μm (Supelco Co., Bellefonte, PA). Sampling was carried out in triplicate. Desorption of volatile compounds trapped on the SPME fiber was performed directly into the GC injector. Volatiles were analyzed by GC−FID as described above. Quantification was performed using individual calibration curves for (*Z*)-hex-3-enal, (*E*)-hex-2-enal, and hexanal by adding known amounts of these compounds to re-deodorized high oleic sunflower oil.

RESULTS AND DISCUSSION

cDNA Cloning and Sequence Analysis of HPL from Olive. On the basis of two highly conserved regions, two degenerate primers were designed from the comparison of known plant HPL amino acid sequences (**Figure 1**). These primers together with an aliquot of an olive cDNA library were used for PCR amplification reactions. The library was made using mRNA isolated from 13 WAF olive fruits, which corresponds to the beginning of oil accumulation in the mesocarp and the seed of the olive fruit, when lignification of the endocarp has taken place. One fragment was obtained with the expected size of about 450 bp. Sequencing of this clone revealed an ORF of 133 amino acids, and the alignment of the deduced amino acid sequence showed a high degree of identity to coding regions of known plant HPL sequences; therefore, it was designated as *OepHPL*.

To obtain the missing 5′ end of the partial cDNA clone, a PCR approach was performed. One reverse gene-specific primer deduced from the 5′ region of the clone and the forward SK primer that binds to the 5′ region of the polylinker of the Uni-ZAP XR vector were used together with an aliquot of the olive cDNA library for PCR amplification. One fragment was amplified, isolated, and sequenced. The sequence showed a 5′ UTR and a start codon (ATG) followed by an ORF matching the 5′ region of the previously known cDNA sequence.

Finally, a specific forward primer deduced from the 5′-UTR sequence of the clone and the reverse T7 primer that binds to the 3′ region of the polylinker of the Uni-ZAP XR vector were used to amplify the corresponding full-length cDNA clone, with an aliquot of the olive cDNA library as the template and a DNA polymerase with proofreading activity to avoid sequencing mistakes because of the amplification. The amplified fragment was isolated, sequenced in both directions, and found to be a full-length cDNA.

The *OepHPL* full-length cDNA clone, with a size of 1641 bp, revealed an ORF encoding a predicted protein of 491 amino acid residues, which corresponds to a calculated molecular mass of 55 kDa and a pI of 7.4. This ORF was flanked by UTRs of 2 bp for the 5′ UTR and 146 bp for the 3′ UTR, with a poly(A) tail at the 3′ end.

The OepHPL amino acid sequence displayed significant similarity to the known plant HPL sequences, exhibiting the highest identity (72%) to the tobacco *NaHPL* gene (AJ414400). Because the similarity with other plant HPLs starts at Leu27, the first 26 amino acids are probably a N-terminal extension (*28*). The lengths of upstream amino acids from this residue are significantly different from other plant HPLs. This N-terminal sequence (**Figure 1**) has structural features of a chloroplast transit peptide, such as the absence of acidic residues and a high proportion of hydroxylated amino acids (*29*). Additionally, two different available programs (PSORT and ProtComp) were used to predict the subcellular localization of the olive HPL protein, and they also indicate a chloroplastic localization of OepHPL. Chloroplast transit peptides have not been identified in all plant HPL sequences, as is the case of those showed in **Figure 1**, except for OepHPL. However, a chloroplastic localization for the HPL protein is admitted because the HPL activity is associated with chloroplasts (*30*) and the targeting of tomato HPL to the outer envelope membrane of chloroplasts has been demonstrated (*31*). As shown in **Figure 1**, OepHPL possesses the four domains (A, B, C, and D) that are highly conserved at the C terminus for many cytochrome P450s (*32*). The D domain contains the absolutely conserved cysteine that serves as a ligand to the heme iron (*28*). A domain typical for enzymes of the cytochrome P450 family was also identified in the olive HPL sequence by National Center for Biotechnology Information (NCBI) Conserved Domain Search and Pfam software.

To elucidate the phylogenetic relationships of the olive HPL gene, its deduced amino acid sequence was included in a dendrogram representing plant HPL sequences for comparison (**Figure 2**). OepHPL was positioned in the group corresponding to dicotyledonous plant HPLs that exhibit strict 13-HPL activity. This establishes OepHPL as a new member of the CYP74B subfamily of the cytochrome P450 (*11*).

Genomic Organization of the Olive HPL Gene. Genomic Southern blot analysis was performed using an OepHPL gene-specific probe corresponding to the 3′-UTR sequence. As displayed in **Figure 3**, one band was observed with olive genomic DNA digested with different restriction enzymes. Because there is not a restriction site for either enzyme within the probe used, these data suggest that at least one copy of *OepHPL* is present in the olive genome.

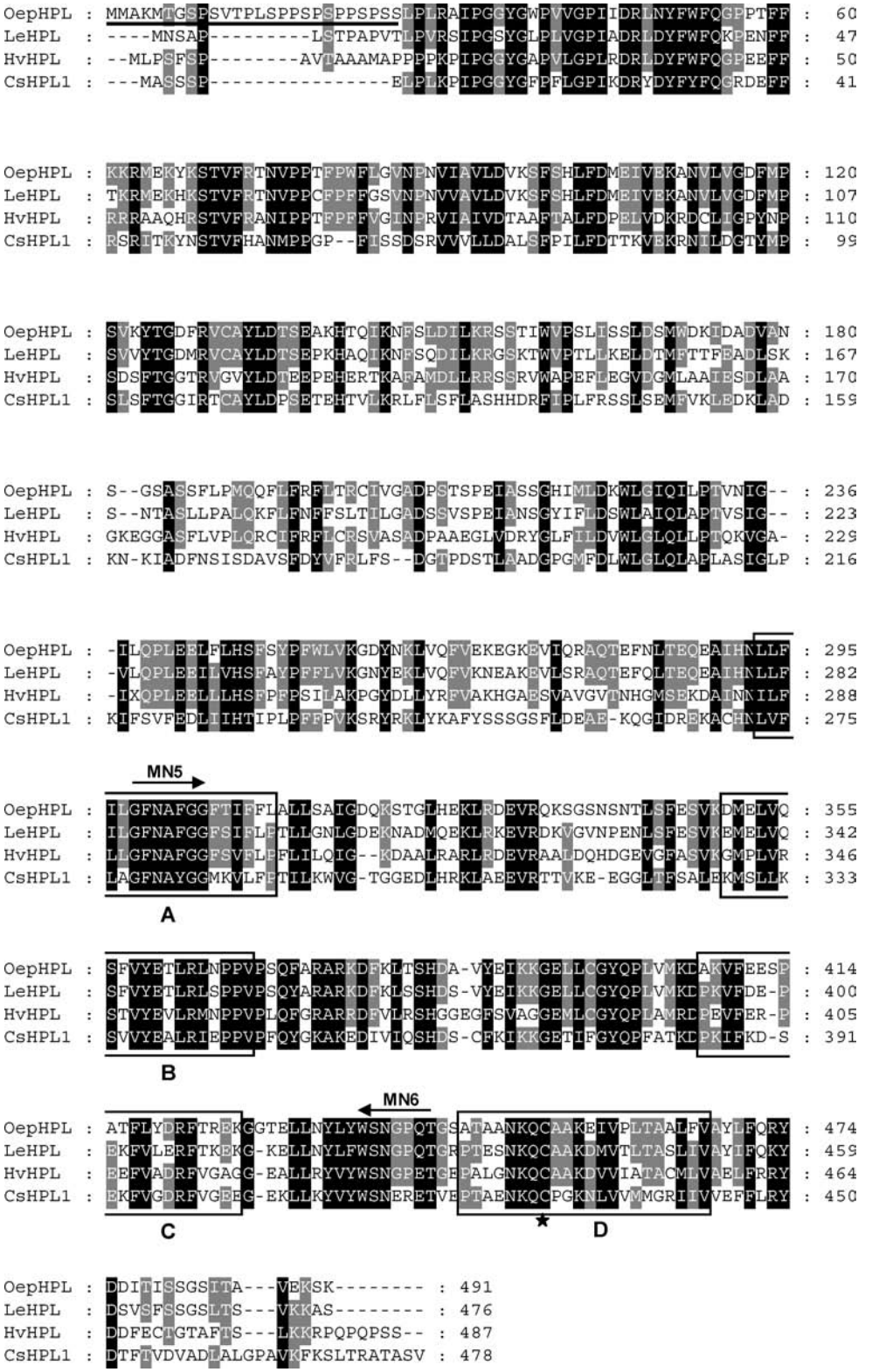

Figure 1. Comparison of the deduced amino acid sequences of olive, tomato, barley, and cucumber *HPL* genes. The sequences were aligned using the ClustalX program and displayed with GeneDoc. Identical and similar residues are shown on a background of black and gray, respectively. The four domains (A, B, C, and D) that are highly conserved at the C terminus for many cytochrome P450s are framed. The conserved cysteine that serves as a ligand to the heme iron is indicated by an asterisk. The sequence of the putative chloroplast transit peptide of OepHPL is underlined. The regions used for deducing degenerate oligonucleotides are denoted by arrows. Accession numbers of the plant HPLs included in the alignment: *Cucumis sativus* (CsHPL1, AF229811), *Hordeum vulgare* (HvHPL, AJ318870), *Lycopersicum esculentum* (LeHPL, AF230372), and *Olea europaea* (OepHPL, EUS13350).

Purification and Biochemical Characterization of the Recombinant Olive HPL. To characterize the biochemical properties of the olive HPL, the corresponding coding region, except the putative transit peptide sequence (**Figure 1**), was placed under the control of an IPTG-inducible promoter of an *E. coli* expression vector. Bacterial cells containing the *OepHPL* overexpression construct

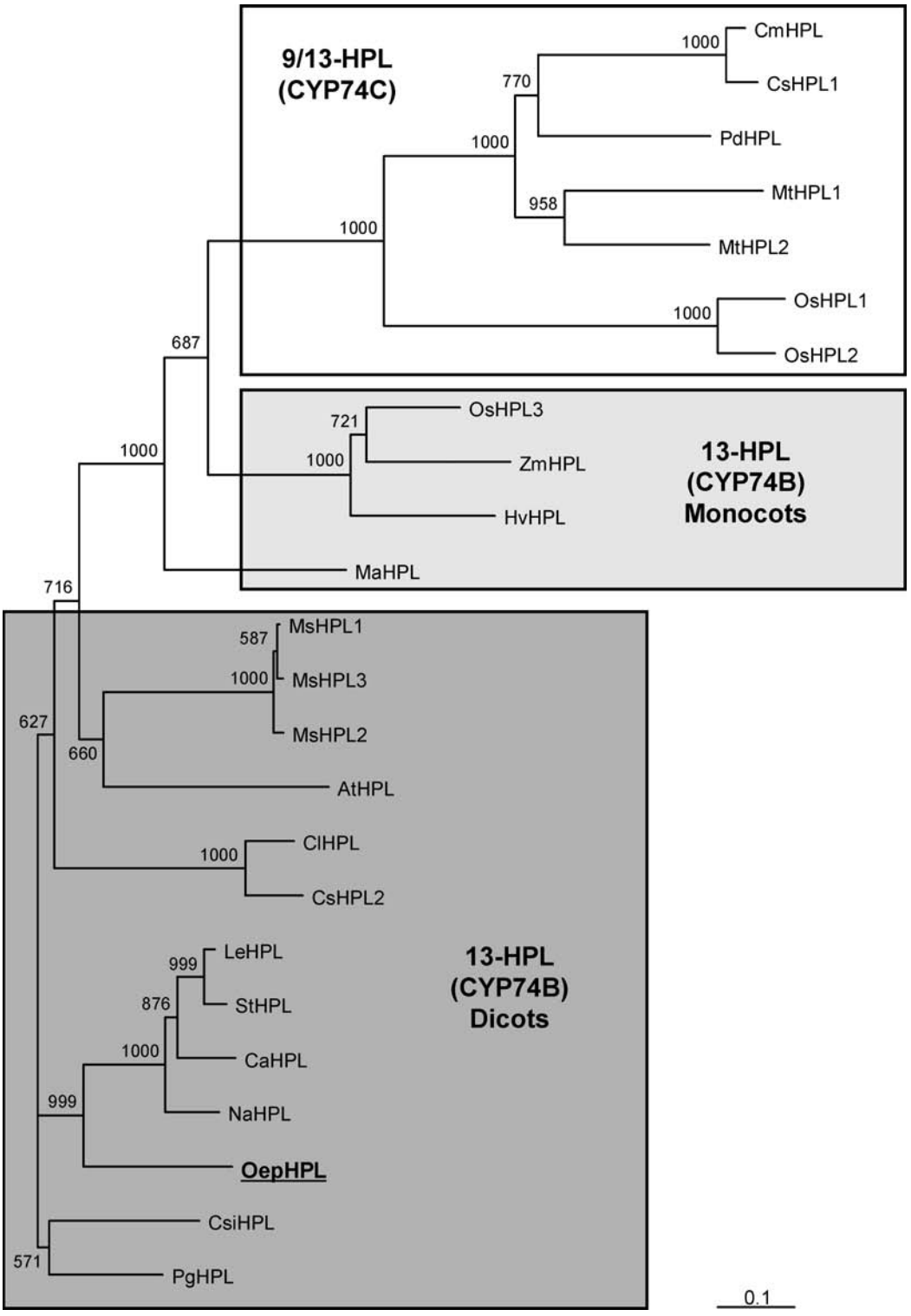

Figure 2. Phylogenetic tree analysis of plant HPLs. Alignments were calculated with ClustalX, and the analysis was performed using the neighbor-joining method implemented in the Phylip package using Kimura's correction for multiple substitutions and a 1000 bootstrap data set. TreeView was used to display the tree. The position of the olive HPL gene isolated in this work is underlined and in bold. Accession numbers of the different HPLs included in the analysis: *Arabidopsis thaliana* (AtHPL, AF087932), *Capsicum annuum* (CaHPL, U51674), *Citrullus lanatus* (ClHPL, AY703450), *Citrus sinensis* (CsiHPL, AY242385), *Cucumis melo* (CmHPL, AF081955), *Cucumis sativus* (CsHPL1, AF229811; CsHPL2, AF229812), *Hordeum vulgare* (HvHPL, AJ318870), *Lycopersicon esculentum* (LeHPL, AF230372), *Medicago sativa* (MsHPL1, AJ249245; MsHPL2, AJ249246; MsHPL3, AJ249247), *Medicago truncatula* (MtHPL1, AJ316562; MtHPL2, AJ316563), *Musa acuminata* (MaHPL, CAB39331), *Nicotiana attenuata* (NaHPL, AJ414400), *Olea europaea* (OepHPL, EUS13350) *Oryza sativa* (OsHPL1, AK105964; OsHPL2, AK107161; OsHPL3, AY340220), *Prunus dulcis* (PdHPL, AJ578748) *Psidium guajava* (PgHPL, AF239670), *Solanum tuberosum* (StHPL, AJ310520), and *Zea mays* (ZmHPL, AY540745).

and grown at 25 °C for 15 h expressed the corresponding T7-tagged protein, which was purified by inmunoaffinity chromatography. Sodium dodecyl sulfate−polyacrylamide gel electrophoresis (SDS−PAGE) analysis (Figure A in the Supporting Information) revealed

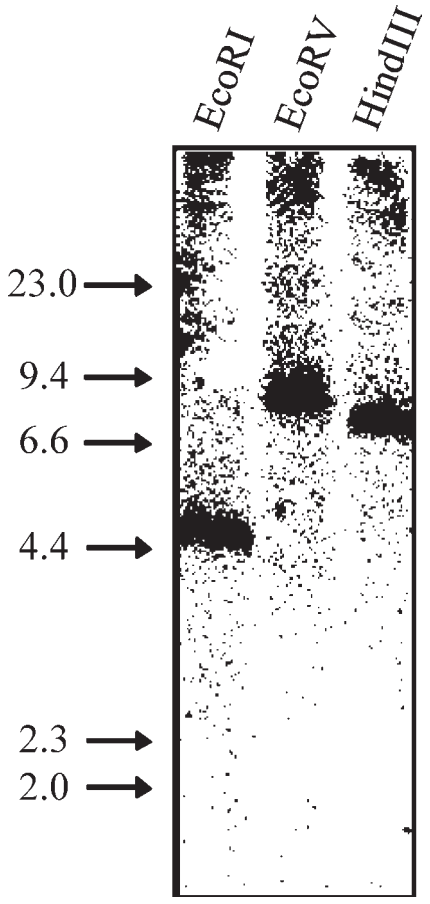

Figure 3. Southern blot analysis of olive genomic DNA digested with the indicated restriction enzymes and probed with *OepHPL* gene-specific probes. The molecular size (kb) of the marker is indicated on the left.

a protein with a molecular mass of about 48 kDa, compatible with the value of 52.4 kDa predicted for the mature protein from the deduced amino acid sequence of the cDNA clone. Crude extracts and purified preparations of these bacteria exhibited HPL activity when 13-LnAOOH or 13-LAOOH was used as the substrate. However, OepHPL presented no activity with 9-LnAOOH or 9-LAOOH, confirming its classification as CYP74B deduced from the phylogenetic tree. To obtain proofs of true HPL activity, reaction products were identified. For this purpose, purified OepHPL was incubated with 13-LnAOOH and 13-LAOOH, and volatile reaction products were trapped on a SPME fiber and analyzed by HRGC−MS. OepHPL products were identified as (*Z*)-hex-3-enal and (*E*)-hex-2-enal when 13-LnAOOH was used as the substrate and as hexanal from 13-LAOOH (Figure B in the Supporting Information). From these results, it is concluded that the *OepHPL* gene encodes a functional 13-HPL and the purified protein was used for its biochemical characterization.

Optimal pH for recombinant OepHPL enzyme activity using 13-LnAOOH as the substrate was measured at 25 °C and various pH values (pH 4.0−10.0). OepHPL displays a broad pH spectrum of enzymatic activity, showing the highest activity at pH 8−9 (**Table 1**). At pH 4, the enzyme possessed 25% remaining activity, whereas at pH 10, it was 80%. Plant HPLs exhibit both acidic and basic optimal pH values, such as cucumber and melon HPLs with optimal pH values of 5.5 and 7.5, respectively (*8*, *33*).

The optimal temperature of recombinant OepHPL activity showed a maximum at 45 °C (**Table 1**). As in the case of optimal pH, activity was observed over a broad interval of temperatures, having more than 50% remaining activity at 15 and 60 °C. Similarly,

Table 1. Properties of Recombinant Olive Fruit OepHPL

substrate	K_m (μM)	V_{max} (nmol min^{-1})	V_{max}/K_m	optimum pH	optimum temperature (°C)
13-LnAOOH	55.7	29.6	0.53	8−9	45
13-LAOOH	47.7	11.6	0.25		

type-2 LOX proteins from olive mesocarp, supplying substrates for this HPL activity, display optimum temperatures at 35 and 45 °C (*17*). However, these type-2 LOX proteins present lower thermal stabilities than HPL. Thus, extraction of VOO at high temperature reduces the availability of substrates for HPL activity because of LOX thermal deactivation, giving rise to oils with lower contents of aroma compounds (*34*).

To study the kinetic properties of recombinant HPLs, enzyme activity was assayed with the ADH/NADH-coupled method over a range of concentrations of the substrates 13-LnAOOH and 13-LAOOH (Figure C in the Supporting Information). The substrate specificities of the recombinant HPL are summarized in **Table 1**. K_m values for 13-LnAOOH and 13-LAOOH of OepHPL were within the value ranges found for other recombinant plant HPLs, such as cucumber, alfalfa, or melon (*8*, *28*, *33*). A comparison of the K_m and V_{max} values revealed that OepHPL had a similar affinity for 13-LnAOOH and 13-LAOOH but cleaved the former substrate about 2.5-fold faster than the latter. The catalytic efficiency (V_{max}/K_m) values of recombinant OepHPL for 13-LnAOOH and 13-LAOOH were 0.53 and 0.24, respectively. These results indicated that 13-LnAOOH was clearly the preferred substrate for OepHPL.

The preferential use of 13-hydroperoxides from polyunsaturated fatty acids as substrates by olive fruit HPL and especially from LnA in concert with the presence of two type-2 LOXs in olive fruit mesocarp (*17*) that can supply these substrates is consistent with the high amounts of C6 compounds that characterize the VOO volatile fraction formed through the LOX pathway. In addition, the absence of 9-HPL activity for the OepHPL enzyme is in agreement with the lack of C9 aldehydes in the VOO volatile fraction, despite the confirmed capacity of olive fruit to generate some 9-hydroperoxides (*15*).

Tissue Specificity and Developmental Expression of the Olive *HPL* Gene. To study the physiological role of the olive *HPL* gene, its expression levels were determined in different olive tissues from Picual and Arbequina varieties using qRT-PCR (**Figure 4**). In both varieties, higher expression levels were observed in leaves compared to young drupes (9 WAF). The mature mesocarp (28 WAF) from the Picual variety showed the highest expression level. These data indicate that *OepHPL* expression is spatially regulated, as reported for the *HPL* gene from *Arabidopsis* (*35*), tomato (*36*), and rough lemon (*37*). Furthermore, temporal regulation might occur according to the differences in the expression levels found in mesocarp tissues of olive fruit with different stages of development. This point was investigated closely by measuring the *OepHPL* gene expression levels in seeds and mesocarp during olive fruit development and ripening of Picual and Arbequina varieties. As shown in **Figure 5A**, very low expression levels of *OepHPL* were detected in seeds from both olive varieties compared to mesocarp, agreeing with the experimental data indicating that no HPL activity is present in seeds (*38*). On the contrary, the *OepHPL* gene is expressed in fruit mesocarp throughout fruit development and ripening, displaying a slight although significant maximum at 23 and 28 WAF in Arbequina and Picual fruits, respectively. These slight maxima preceded the fruit developmental stage, which gives rise to oils with the highest contents of C6 aldehydes in both varieties (**Figure 5B**). Temporal regulation of the *HPL* gene expression was also described during

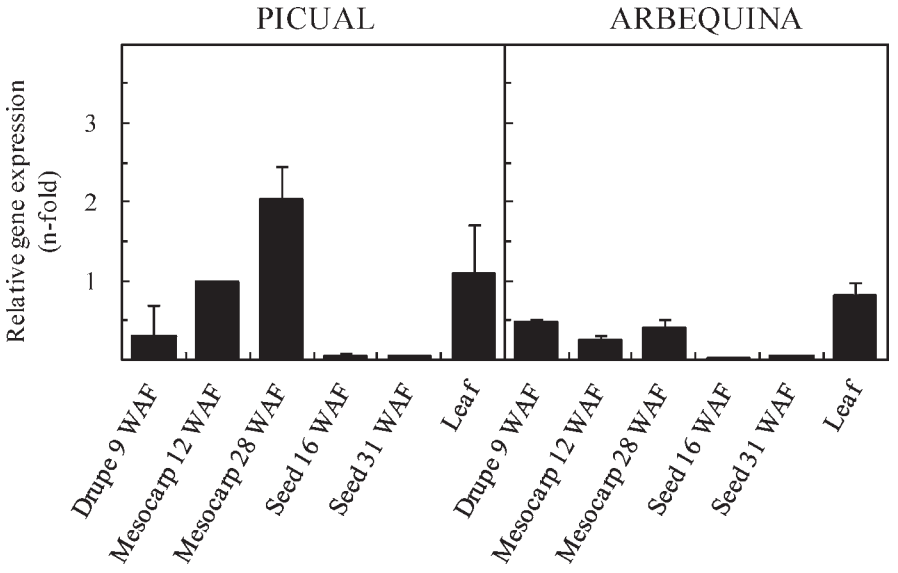

Figure 4. Relative expression levels of *OepHPL* gene in different tissues of Picual and Arbequina varieties. Data represent means ± SD of three reactions performed in duplicate as described in the Materials and Methods.

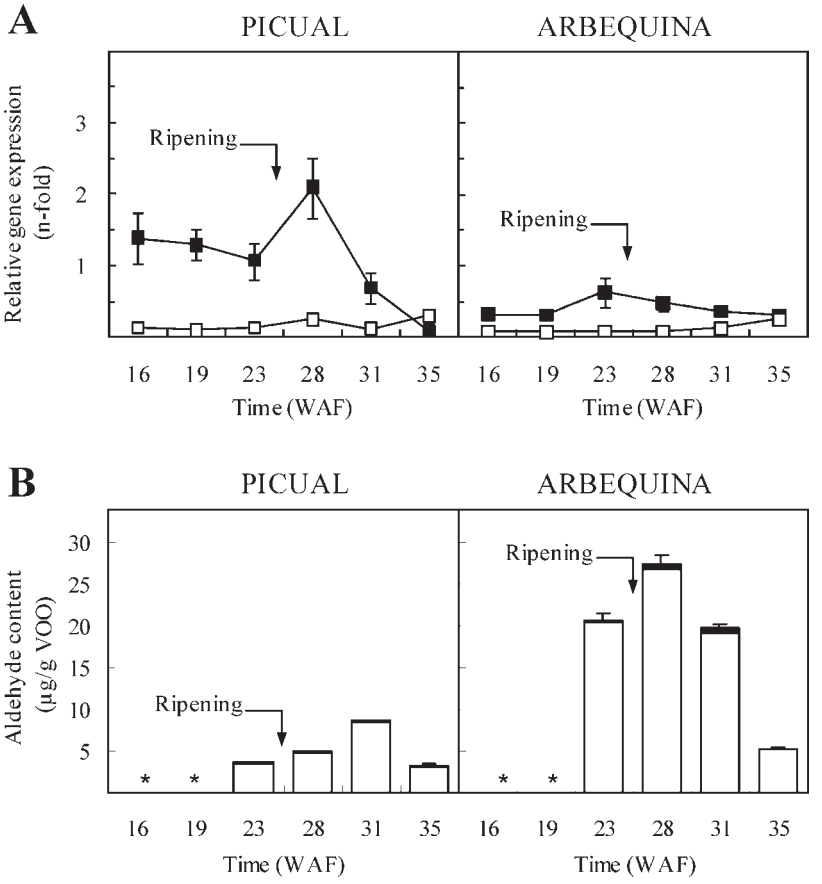

Figure 5. (A) Changes of expression levels of *OepHPL* gene in mesocarp tissue (■) or seeds (□) of Picual and Arbequina varieties during olive fruit development and ripening and (B) changes of contents of hexenals [(*Z*)-hex-3-enal + (*E*)-hex-2-enal] (white bars) and hexanal (black bars) in the corresponding VOOs. Data on expression levels represent means ± SD of three reactions performed in duplicate as described in the Materials and Methods. Data on hexenal and hexanal contents represent means ± SD of two oils analyzed in triplicate as described in the Materials and Methods. (*) No oil could be obtained from 16 and 19 WAF olive fruits by means of the Abencor analyzer because of the low oil yield.

tomato fruit development and ripening (*36*). Changes of *OepHPL* gene expression levels are quantitatively different from those observed for the main olive *LOX* gene involved in the biosynthesis of VOO aroma compounds (*Oep2LOX2*) that increases up to 300-fold in Picual fruits at ripening (*17*), so that the synthesis of C6 compounds in VOO followed quite a similar profile to that of *Oep2LOX2* gene expression. It is noteworthy to mention that, in potato leaf chloroplasts, a metabolic interaction between a specific 13-LOX and a 13-HPL has been proposed (*12*). *OepHPL* expression levels detected in mesocarp might be sufficient to

supply enough HPL activity to metabolize the 13-hydroperoxides generated by olive type-2 LOXs. However, preliminary work on factors affecting VOO aroma synthesis (data not shown) points to HPL activity as a limiting factor for this synthesis. This limitation seems to affect especially the C6 aldehyde synthesis in Arbequina fruit in good agreement with the significantly lower *OepHPL* expression levels observed in Arbequina fruit in comparison to Picual fruit (**Figure 5A**), despite the fact that Arbequina olive oils have higher C6 aldehyde contents than Picual olive oils. This apparent contradiction might be explained by numerous factors, either biochemical or technological, that can modify the HPL activity level originally present in the fruit during oil extraction, such as the inactivation by oxidized phenolics arising during this industrial process, which depends upon the variety. In this sense, the inactivating role of oxidized phenolics on enzyme activity is well-established (*39*), and olive seed peroxidase activity might also act as a major factor oxidizing olive phenolics (*40*).

In conclusion, the isolation and functional characterization of a *HPL* gene from olive fruit has been carried out. Sequence analysis of the *OepHPL* gene shows that it codes for a 13-HPL protein. Genomic Southern blot data are consistent with the presence of at least one copy of the *HPL* gene in the olive genome. The identity of the *HPL* gene was confirmed by functional expression in bacteria. Kinetic studies show that 13-LnAOOH is the preferred substrate for recombinant olive HPL and that it produces (*Z*)-hex-3-enal, which isomerizes partially to (*E*)-hex-2-enal from 13-LnAOOH and hexanal from 13-LAOOH, in good agreement with the composition of VOO aroma. *OepHPL* expression is spatially and temporally regulated in olive fruit during development and ripening. All of these data point out the involvement of OepHPL in the biosynthesis of aroma compounds of VOO.

ACKNOWLEDGMENT

We thank Dr. D. G. Richardson for critical reading of the manuscript.

Supporting Information Available: Gene accession numbers and sequences of primer pairs used for gene expression analysis by qRT-PCR in the present study (Table A), SDS−PAGE of purified recombinant olive HPL (Figure A), HRGC−MS analysis of the reaction products of OepHPL (Figure B), and effect of the substrate concentration on OepHPL enzymatic activity (Figure C). This material is available free of charge via the Internet at http://pubs.acs.org.

LITERATURE CITED

(1) Prost, I.; Dhondt, S.; Rothe, G.; Vicente, J.; Rodriguez, M. J.; Kift, N.; Carbonne, F.; Griffths, G.; Esquerre-Tugaye, M. T.; Rosahl, S.; Castresana, C.; Hamberg, M.; Fournier, J. Evaluation of the antimicrobial activities of plant oxylipins supports their involvement in defense against pathogens. *Plant Physiol.* **2005**, *139*, 1902–1913.

(2) Vancanneyt, G.; Sanz, C.; Farmaki, T.; Paneque, M.; Ortego, F.; Castañera, P.; Sánchez-Serrano, J. J. Hydroperoxide lyase depletion in transgenic potato plants leads to an increase in aphid performance. *Proc. Natl. Acad. Sci. U.S.A.* **2001**, *98*, 8139–8144.

(3) Arimura, G.; Kost, C.; Boland, W. Herbivore-induced, indirect plant defences. *Biochim. Biophys. Acta* **2005**, *1734*, 91–111.

(4) Noordermeer, M. A.; Veldink, G. A.; Vliegenthart, J. F. Fatty acid hydroperoxide lyase: A plant cytochrome P450 enzyme involved in wound healing and pest resistance. *ChemBioChem* **2001**, *2*, 494–504.

(5) Matsui, K.; Toyota, H.; Kajiwara, T.; Kakuno, T.; Hatanaka, A. Fatty acid hydroperoxide cleaving enzyme, hydroperoxide lyase, from tea leaves. *Phytochemistry* **1991**, *30*, 2109–2113.

(6) Fukushige, H.; Hildebrand, D. F. Watermelon (*Citrullus lanatus*) hydroperoxide lyase greatly increase C6 aldehyde formation in transgenic leaves. *J. Agric. Food Chem.* **2005**, *53*, 2046–2051.

(7) Fauconnier, M.-L.; Perez, A. G.; Sanz, C.; Marlier, M. Purification and characterization of tomato leaf (*Licopersicon esculentum* Mill.) hydroperoxide lyase. *J. Agric. Food Chem.* **1997**, *45*, 4232–4236.

(8) Matsui, K.; Ujita, C.; Fujimoto, S.-H.; Wilkinson, J.; Hiatt, B.; Knauf, V.; Kajiwara, T.; Feussner, I. Fatty acid 9- and 13-hydroperoxide lyases from cucumber. *FEBS Lett.* **2000**, *481*, 183–188.

(9) Noordermeer, M. A.; Veldink, G. A.; Vliegenthart, J. F. G. Alfalfa contains substantial 9-hydroperoxide lyase activity and a 3*Z*:2*E*-enal isomerase. *FEBS Lett.* **1999**, *443*, 201–204.

(10) Kim, I.-S.; Grosch, W. Partial purification and properties of a hydroperoxide lyase from fruits of pear. *J. Agric. Food Chem.* **1981**, *29*, 1220–1225.

(11) Stumpe, M.; Feussner, I. Formation of oxylipins by CYP74 enzymes. *Phytochem. Rev.* **2006**, *5*, 347–357.

(12) Farmaki, T.; Sanmartín, M.; Jiménez, P.; Paneque, M.; Sanz, C.; Vancanneyt, G.; León, J.; Sánchez-Serrano, J. J. Differential distribution of the lipoxygenase pathway enzymes within potato chloroplasts. *J. Exp. Bot.* **2007**, *58*, 555–568.

(13) Morales, M. T.; Aparicio, R; Ríos, J. J. Dynamic headspace gas chromatographic method for determining volatiles in virgin olive oil. *J. Chromatogr., A* **1994**, *668*, 455–462.

(14) Angerosa, F.; Mostallino, R.; Basti, C.; Vito, R. Virgin olive oil odour notes: Their relationships with the volatile compound from the lipoxygenase pathway and secoiridoid compounds. *Food Chem.* **2000**, *68*, 283–287.

(15) Olías, J. M.; Pérez, A. G.; Rios, J. J.; Sanz, C. Aroma of virgin olive oil: Biogenesis of the green odor notes. *J. Agric. Food Chem.* **1993**, *41*, 2368–2373.

(16) Salas, J. J.; Williams, M.; Harwood, J. L.; Sánchez, J. Lipoxygenase activity in olive (*Olea europaea*) fruit. *J. Am. Oil Chem. Soc.* **1999**, *76*, 1163–1169.

(17) Padilla, M. N.; Hernandez, M. L.; Sanz, C.; Martinez-Rivas, J. M. Functional characterization of two 13-lipoxygenase genes from olive fruit in relation to the biosynthesis of volatile compounds of virgin olive oil. *J. Agric. Food Chem.* **2009**, *57*, 9097–9107.

(18) Salas, J. J.; Sánchez, J. Hydroperoxide lyase from olive (*Olea europaea*) fruits. *Plant Sci.* **1999**, *143*, 19–26.

(19) Sánchez-Ortiz, A.; Pérez, A. G.; Sanz, C. Cultivar differences on nonesterified polyunsaturated fatty acid as a limiting factor for biogenesis of virgin olive oil aroma. *J. Agric. Food Chem.* **2007**, *55*, 7869–7873.

(20) Haralampidis, K.; Milioni, D.; Sánchez, J.; Baltrusch, M.; Heinz, E.; Hatzopoulos, P. Temporal and transient expression of stearoyl-ACP carrier protein desaturase gene during olive fruit development. *J. Exp. Bot.* **1998**, *49*, 1661–1669.

(21) Hernández, M. L.; Mancha, M.; Martínez-Rivas, J. M. Molecular cloning and characterization of genes encoding two microsomal oleate desaturases (*FAD2*) from olive. *Phytochemistry* **2005**, *66*, 1417–1426.

(22) Murray, M. G.; Thomson, W. F. Rapid isolation of high weight plant DNA. *Nucleic Acid Res.* **1980**, *8*, 4321–4325.

(23) Hernández, M. L.; Padilla, M. N.; Mancha, M.; Martínez-Rivas, J. M. Expression analysis identifies *FAD2-2* as the olive desaturase gene mainly responsible for the linoleic acid content in virgin olive oil. *J. Agric. Food Chem.* **2009**, *57*, 6199–6206.

(24) Livak, K. J.; Schmittgen, T. D. Analysis of relative gene expression data using real-time quantitative PCR and the $2^{-\Delta\Delta Ct}$ method. *Methods* **2001**, *25*, 402–408.

(25) Vick, B. A. A spectrometric assay for hydroperoxide lyase. *Lipids* **1991**, *26*, 315–320.

(26) Hamberg, M.; Samuelsson, B. On the specificity of the oxygenation of unsaturated fatty acids catalyzed by soybean lipoxygenase. *J. Biol. Chem.* **1967**, *242*, 5329–5335.

(27) Galliard, T.; Phillips, D. R. Lipoxygenase from potato tubers. *Biochem. J.* **1971**, *124*, 431–438.

(28) Noordermeer, M. A.; van Dijken, A. J. H.; Smeekens, S. C. M.; Veldink, G. A.; Vliegenthart, J. F. G. Characterization of three cloned and expressed 13-hydroperoxide lyase isoenzymes from

alfalfa with unusual N-terminal sequences and different enzyme kinetics. *Eur. J. Biochem.* **2000**, *267*, 2473–2482.
(29) Fuks, B; Schnell, D. J. Mechanism of protein transport across the chloroplast envelope. *Plant Physiol.* **1997**, *114*, 405–410.
(30) Blée, E; Joyard, J. Envelope membranes from spinach chloroplasts are a site of metabolism of fatty acid hydroperoxides. *Plant Physiol.* **1996**, *110*, 445–454.
(31) Froehlich, J. E.; Itoh, A.; Howe, G. A. Tomato allene oxide synthase and fatty acid hydroperoxide lyase, two cytochrome P450s involved in oxylipin metabolism, are targeted to different membranes of chloroplast envelope. *Plant Physiol.* **2001**, *125*, 306–317.
(32) Bate, N. J.; Sivasankar, S.; Moxon, C.; Riley, J. M. C.; Thompson, J. E.; Rothstein, S. J. Molecular characterization of an *Arabidopsis* gene encoding hydroperoxide lyase, a cytochrome P-450 that is wound inducible. *Plant Physiol.* **1998**, *117*, 1393–1400.
(33) Tijet, N.; Schneider, C.; Muller, B. L.; Brash, A. R. Biogenesis of volatile aldehydes from fatty acid hydroperoxides: Molecular cloning of a hydroperoxide lyase (CYP74C) with specificity for both the 9- and 13-hydroperoxides of linoleic and linolenic acids. *Arch. Biochem. Biophys.* **2001**, *386*, 281–289.
(34) Luaces, P.; Sanz, C.; Pérez, A. G. Thermal stability of lipoxygenase and hydroperoxide lyase from olive fruit and repercussion on olive oil aroma biosynthesis. *J. Agric. Food Chem.* **2007**, *55*, 6309–6313.
(35) Matsui, K; Wilkinson, J.; Hiatt, B.; Kauf, V.; Kajiwara, T. Molecular cloning and expression of *Arabidopsis* fatty acid hydroperoxide lyase. *Plant Cell Physiol.* **1999**, *40*, 477–481.
(36) Howe, G. A.; Lee, G. I.; Itoh, A.; Li, L.; De Rocher, A. E. Cytochrome P450-dependent metabolism of oxylipins in tomato. Cloning and expression of allene oxide synthase and fatty acid hydroperoxide lyase. *Plant Physiol.* **2000**, *123*, 711–724.
(37) Gomi, K.; Yamasaki, Y.; Yamamoto, Y.; Akimitsu, K. Characterization of a hydroperoxide lyase gene and effect of C_6-volatiles on expression of genes of the oxylipin metabolism in *Citrus*. *J. Plant Physiol.* **2003**, *160*, 1219–1231.
(38) Luaces, P.; Pérez, A. G.; Sanz, C. Role of olive seed in the biogenesis of virgin olive oil aroma. *J. Agric. Food Chem.* **2003**, *51*, 4741–4745.
(39) Loomis, W. D.; Battaille, J. Plant phenolic compounds and the isolation of plant enzymes. *Phytochemistry* **1966**, *5*, 423–438.
(40) Luaces, P.; Romero, C.; Gutiérrez, F.; Sanz, C.; Pérez, A. G. Contribution of olive seed to the phenolic profile and related quality parameters of virgin olive oil. *J. Sci. Food Agric.* **2007**, *87*, 2721–2727.

Received for review December 23, 2009. Revised manuscript received March 11, 2010. Accepted March 13, 2010. This work was supported by research projects AGL2008-00258 from Programa Nacional de Recursos y Tecnologías Alimentarias funded by the Spanish Government and P06-AGR-02151 from Incentivos a Proyectos de Investigación de Excelencia funded by the Andalusian Government. M.N.P. and M.L.H. are recipients of Formación de Personal Investigador (FPI) fellowships from Junta de Andalucía.